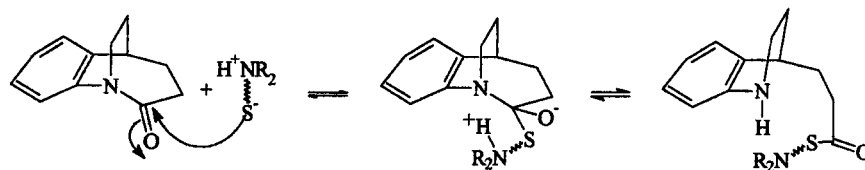


Scheme 1



^1H NMR and ^{13}C NMR spectra were obtained using a Bruker WH-200 or a Bruker AM-400 spectrometer. Infrared spectra were recorded using a Nicolet Magna 750 FTIR spectrometer. High-resolution mass spectra were obtained using an AEI-MS50 mass spectrometer and low-resolution spectra using an AEI-MS12 spectrometer.

Flash chromatography was performed using silica gel 60 (Merck, 40–63 μm particle size).

(B) Kinetics. The following buffers were used to control the pH: HCl, acetic acid ($\text{p}K_{\text{a}}$ 4.76), MES ($\text{p}K_{\text{a}}$ 6.1), *N*-methylimidazole ($\text{p}K_{\text{a}}$ 6.95), MOPS ($\text{p}K_{\text{a}}$ 7.2), phosphate ($\text{p}K_{\text{a}}$ 7.2), *N*,2-dimethylimidazole ($\text{p}K_{\text{a}}$ 7.4), HEPES ($\text{p}K_{\text{a}}$ 7.5), and CHES ($\text{p}K_{\text{a}}$ 9.3). For studies involving the reaction of thioglycolic acid with amide **1** at pH's near 4 and 10, thioglycolic acid itself was used as the buffer ($\text{p}K_1 = 3.55$, $\text{p}K_2 = 10.22^b$). Buffers were made using purified, deoxygenated H_2O from an Osmonics Aries water purification system ($\mu = 1.0$ (KCl)) and were further degassed by bubbling Ar through them for several hours before use.

The rate of ring opening of the strained amide **1** in the presence of excess thiol was followed by observing the increase in absorbance at 291 nm (250 nm at pH 4, and 270 nm at pH 3.55 for thioglycolic acid reactions). At lower pH (2–3) the reaction was followed by observing the decrease in absorbance at 230 and 240 nm. Reactions were followed using a modified Cary 17 UV–vis spectrophotometer interfaced to an IBM 486 PC fitted with Olis software (Online Instrument Systems, Jefferson Ga., 1992) or an Applied Photophysics Sequential Stopped Flow Spectrophotometer interfaced with an Acorn A5000 RISC OS desktop computer. In the cases of conventional spectroscopy 3 mL of deoxygenated buffer was transferred via syringe to Ar flushed quartz cells, followed by addition of a concentrated stock solution of the thiol in water or CH_3CN to give final concentrations of 0.1–15 mM (up to 3% CH_3CN). The cells were equilibrated in the spectrophotometer cell holder at 25.0 $^\circ\text{C}$ for 10 min after which the reaction was initiated by injection of 5–10 μL of a 0.08 M stock solution of amide **1** in dry CH_3CN . An excess of thiol of at least 10-fold was used so that the reactions were pseudo-first order in all cases. Reactions were followed to at least 5 half-times. Pseudo-first-order rate constants (k_{obs}) were obtained for each run by nonlinear least-squares (NLLSQ) fitting of the absorbance vs time data to a standard exponential model ($A_t = A_{\infty} + (A_0 - A_{\infty}) \exp(-k_{\text{obs}}t)$). The final pH of the cells was measured after each run (to ensure constancy of pH) using a Radiometer VIT 90 Video Titrator equipped with a GK2321C combination electrode standardized by Fisher certified pH 4.00, 7.00, and 10.00 buffers. Second-order rate constants (k_2^{obs}) for the reaction of thiols with amide **1** were obtained from the slopes of plots of k_{obs} vs $[\text{thiol}]_T$ at each pH (3–4 concentrations). For the reactions of amide with thioglycolic acid in the pH region of 3–4 and 9–11, thioglycolate itself was used as the buffer. In these cases, the buffers were made up to the desired final concentrations (15–200 mM) by addition of thoroughly deoxygenated water to sodium thioglycolate and KCl in a volumetric flask, followed by rapid adjustment of the pH using concentrated NaOH or HCl (O_2 free conditions). Three milliliters of the buffer solutions was then syringed into serum stoppered quartz cells and runs were carried out as above.

Thiol compounds and their stock solutions were titrated periodically using either iodometric titration^{6a} or reaction with Ellman's reagent^{6b,c} (5,5'-dithiobis(2-nitrobenzoic acid)) in order to monitor the amount of air oxidation of thiol to disulfide. In the experiments with low thiol concentrations, titration with Ellman's reagent was used to determine the exact concentration of thiol in the reaction mixture. The second-order rate constants obtained from the above experiments over the range

Table 1. Second-Order Rate Constants Measured at Various pH Values for the Reaction of Thioglycolic Acid (**2**) with Amide **1** ($T = 25.0$ $^\circ\text{C}$, $\mu = 1.0$ (KCl))

pH	buffer	concn (M)	k_2^{obs} ($\text{M}^{-1} \text{s}^{-1}$) ^a
2.02	HCL	9.5×10^{-3}	1.46 ± 0.15
2.19	HCL	6.5×10^{-3}	1.38 ± 0.17
3.43	thioglycolic acid	0.05–0.20	1.72 ± 0.10
4.00	thioglycolic acid	0.05–0.20	1.60 ± 0.15
4.50	acetate	0.05	1.78 ± 0.18
5.16	acetate	0.20	1.41 ± 0.02
5.40	MES	0.05	1.52 ± 0.15
5.90	MES	0.05	1.35 ± 0.04
7.00	MOPS	0.05	1.73 ± 0.17
7.08	phosphate	0.20	1.69 ± 0.18
7.20	1,2-dimethylimidazole	1.0	1.33 ± 0.08
7.94	HEPES	0.05	1.65 ± 0.15
8.20	HEPES	0.20	1.46 ± 0.08
9.00	CHES	0.05	1.86 ± 0.04
9.75	thioglycolic acid	0.05–0.20	0.83 ± 0.01
10.06	thioglycolic acid	0.05–0.20	0.78 ± 0.06
10.47	thioglycolic acid	0.05–0.20	0.27 ± 0.06
10.50	thioglycolic acid	0.05–0.20	0.432 ± 0.003
10.90	thioglycolic acid	0.05–0.20	0.24 ± 0.03

^a k_2^{obs} determined from the slope of a plot of k_{obs} vs $[\text{thiol}]_T$ at each pH (4 different thiol concentrations). The quoted error in k_2^{obs} is the standard deviation in the slope calculated by the linear regression fitting.

Table 2. Second-Order Rate Constants Measured at Various pH Values for the Reaction of Ethyl 2-Mercaptoacetate (**3**) with Amide **1** ($T = 25.0$ $^\circ\text{C}$, $\mu = 1.0$ (KCl))

pH	buffer	concn (M)	k_2^{obs} ($\text{M}^{-1} \text{s}^{-1}$) ^a
4.51	acetate	1.0	0.36 ± 0.02
6.16	MES	0.20	0.34 ± 0.03
6.89	MOPS	0.20	0.32 ± 0.01
7.65	MOPS	0.20	0.24 ± 0.02
8.05	HEPES	0.20	0.155 ± 0.007

^a k_2^{obs} determined from the slope of a plot of k_{obs} vs $[\text{thiol}]_T$ at each pH (4 different concentrations). The quoted error in k_2^{obs} is the standard deviation in the slope calculated by the linear regression fitting.

Table 3. Second-Order Rate Constants Measured at Various pH Values for the Reaction of (Dimethylamino)ethanethiol (**5**) with Amide **1** ($T = 25.0$ $^\circ\text{C}$, $\mu = 1.0$ (KCl))

pH	buffer	concn (M)	k_2^{obs} ($\text{M}^{-1} \text{s}^{-1}$) ^a
4.54	acetate	0.1	0.26 ± 0.01
4.54	acetate	1.0	0.27 ± 0.02
5.15	acetate	0.2	0.39 ± 0.007
6.25	MES	0.05	0.93 ± 0.013
7.15	MOPS	0.05	5.17 ± 0.05
7.98	MOPS	0.05	20.3 ± 0.5
8.39	TAPS	0.05	25.3 ± 0.7
9.33	CHES	0.05	29.3 ± 1.0

^a k_2^{obs} determined from the slope of a plot of k_{obs} vs $[\text{thiol}]_T$ at each pH (4 different thiol concentrations). The quoted error in k_2^{obs} is the standard deviation in the slope calculated by the linear regression fitting.

of pH 2–11 are given in Table 1. Given in Tables 2 and 3 are the rate constants for the reaction of **1** with ethyl thioglycolate **3** and (dimethylamino)ethanethiol (**5**, dimethylcysteamine).

(C) Product Studies. (1) Amide 1 + Thioglycolic Acid (2). In an attempt to isolate the product of reaction of amide **1** with thioglycolic acid, a large-scale reaction was carried out in pH 7 phosphate buffer

(6) (a) Street, J. P.; Skorey, K. I.; Brown, R. S.; Ball, R. G. *J. Am. Chem. Soc.* **1985**, *107*, 7669–7679. (b) Ellman, G. L. *Arch. Biochem. Biophys.* **1959**, *82*, 70–77. (c) Habeeb A. *Methods Enzymol.* **1972**, *457*–464.

under conditions identical to those used in the kinetic runs ($T = 25$ °C, $\mu = 1.0$ (KCl)).

To a 200-mL volumetric flask was added 0.0767 g (0.41 mmol) of amide in 6 mL of CH_3CN followed by 0.53 g (4.6 mmol) of sodium thioglycolate. The solution was diluted to volume with pH 7.08 phosphate buffer (0.200 M, $\mu = 1.0$ (KCl)) (solution was somewhat cloudy). The solution was stirred for 7.5 min (~ 25 half times, where $t_{1/2} = \ln 2 / (k_2^{\text{obs}}[\text{thiol}]_T)$) and then 6 M HCl was added dropwise to bring the solution to pH 4.8. The aqueous solution was extracted with 3×60 mL of EtOAc and the combined extracts were dried over CaCl_2 . After filtration and evaporation of the solvent, 0.049 g of a yellow oil remained. Spectral data indicated that the major component isolated was thioester **4a**, $R = \text{H}$. The characteristic carbonyl resonance for a thiol ester⁷ was observed at 197.58 ppm in the ^{13}C spectrum as expected. Extra peaks present in the ^{13}C and ^1H NMR spectra not assignable to the thiol ester can be attributed to thioglycolic acid or its disulfide which were coextracted into the EtOAc. IR ($\text{CH}_2\text{Cl}_2/\text{MeOH}$ cast film) ν 3100–2400 (NH_2^+), 1692 ($\text{SC}=\text{O}$), 1603/1381 ($-\text{COO}^-$), 1578, 1287, 1192 cm^{-1} ; ^1H NMR (400 MHz, CD_3OD) δ 1.65–2.05 (m, 4H, contains both NCH_2CH_2 and $\text{CHCH}_2\text{CH}_2\text{C}=\text{O}$), 2.61–2.70 (m, 2H, $\text{CH}_2\text{CH}_2\text{C}=\text{O}$), 2.71–2.80 (m, 1H, benzylic CH), 3.20 (s, of $\text{HS}-\text{CH}_2-\text{COOH}$ or disulfide impurity), 3.13–3.32 (m, 2H, NCH_2CH_2), 3.30 (s, $\text{HS}-\text{CH}_2-\text{COOH}$ or disulfide impurity), 3.70 (s, 2H, $\text{SCH}_2\text{C}=\text{O}$), 6.56 (d/d, $J = 1.0$, 7.5 Hz, 1H), 6.62 (t/d, $J = 1.0$, 7.5 Hz, 1H), 6.92 (t/d, $J = 1.0$, 7.5 Hz, 1H), 6.98 (d, $J = 7.5$ Hz, 1H); ^{13}C NMR (75 MHz, CDCl_3) δ 25.55 (CH_2), 26.48 (CH_2 , thioglycolic acid), 31.35 (CH_2), 31.42 (CH_2), 34.22 (CH), 38.85 (CH_2), 40.94 (CH_2), 117.39 (CH), 120.87 (CH), 127.00 (quat C), 127.47 (CH), 129.32 (CH), 140.06 (quat C), 174.02 ($\text{C}=\text{O}$, carboxylate), 176.32 ($\text{C}=\text{O}$, thioglycolic acid), 197.58 ($\text{C}=\text{O}$, thiol ester); HRMS (EI), exact mass calcd for $\text{C}_{14}\text{H}_{17}\text{O}_3\text{N}_1\text{S}_1$ 279.0929, found 279.0921 (2.92%).

(2) Amide (1) + Ethyl 2-Mercaptoacetate (3). To 26 mg (0.14 mmol) of amide in a 200-mL volumetric flask was added 6 mL of CH_3CN and 12 equiv (1.73 mmol) of $\text{HSCH}_2\text{COOEt}$. The flask was quickly diluted to volume with deoxygenated water, and timing was started. The solution pH was adjusted to 7 with 4 M NaOH, and the reaction was allowed to proceed for 7 half times (based on $k_2^{\text{obs}} = 0.34 \text{ M}^{-1} \text{ s}^{-1}$ for the reaction of **1** and **3** at this pH). The reaction mixture was then worked up as above (except that MgSO_4 was used as a drying agent), giving 22 mg of a yellow oil.

The ^1H NMR spectrum corresponded to that of authentic **4b**, $R = \text{Et}$, synthesized by an independent route (see below) + coextracted disulfide ($\text{EtOC(O)CH}_2\text{SSCH}_2\text{C(O)OEt}$). IR (CH_2Cl_2 cast film) ν 3409 (NH), 2980, 2932, 2857, 1735 ($\text{C}=\text{O}$, O ester), 1695 ($\text{C}=\text{O}$, thiol ester), 1606, 1500, 1297, 1268 cm^{-1} ; ^{13}C (75 MHz, CDCl_3) δ 14.13 (CH_3), 26.19 (CH_2), 31.34 (CH_2), 31.63 (CH_2), 34.77 (CH_2), 38.24 (CH_2), 41.22 (CH_2), 61.87 (CH_2), 114.27 (CH), 116.78 (CH), 123.66 (quat C), 127.25 (CH), 129.17 (CH), 144.22 (quat C), 168.77 ($\text{C}=\text{O}$, ester), 197.46 ($\text{C}=\text{O}$, thiol ester). Extra peaks in the ^{13}C spectrum were identified as the disulfide of ethyl 2-mercaptoacetate; δ 14.18 ($-\text{CH}_3$), 41.53 ($-\text{CH}_2-\text{SS}-\text{CH}_2-$), 61.71 ($-\text{CH}_2-\text{O}-$), 169.37 ($\text{C}=\text{O}$). HRMS (EI), exact mass calcd for $\text{C}_{16}\text{H}_{21}\text{O}_3\text{N}_1\text{S}_1$ 307.1242, found 307.1244 (31%).

(3) Synthesis of Thio Ester 4b, R = Et, by an Independent Route. To 3 mL of dry CH_3CN was added **1** (50 mg, 0.267 mmol), ethyl 2-mercaptoacetate (0.29 mL, 10 equiv), and dry triethylamine (1 mL, 2.7 equiv). After 24 h of stirring at room temperature under Ar, the volatiles were removed under vacuum (1 mmHg) and the resulting gum was triturated with hexane (3×25 mL) to remove the thio ester. The hexane solutions were combined and hexane removed to yield an oily yellowish product. This oil was dissolved in CH_2Cl_2 and washed several times with H_2O (3×50 mL) to further remove any contaminating thiolate or triethylammonium thiolate. The CH_2Cl_2 solution was dried over MgSO_4 , and the CH_2Cl_2 removed in vacuum giving a yellowish oil. This oil was further purified by preparative TLC (Silica Gel 60 F₂₅₄ plates, 50 EtOAc/50 hexane) to give about 13 mg of product with the following characteristics: IR (CH_2Cl_2 cast film) ν 3410, 2979, 2928, 2856, 1737, 1694, 1606, 1500, 1474, 1298, 1264 cm^{-1} ; ^1H NMR (400 MHz, CDCl_3) δ 1.28 (t, 3H, CH_2CH_3), 1.74–1.81 (m, 1H), 1.87–1.99 (m, 2H), 2.03–2.12 (m, 1H), (last three signals contain both NCH_2CH_2 and $\text{CHCH}_2\text{CH}_2\text{C}=\text{O}$ protons), 2.66–2.75 (m, 2H, $\text{CH}_2\text{C}=\text{O}$),

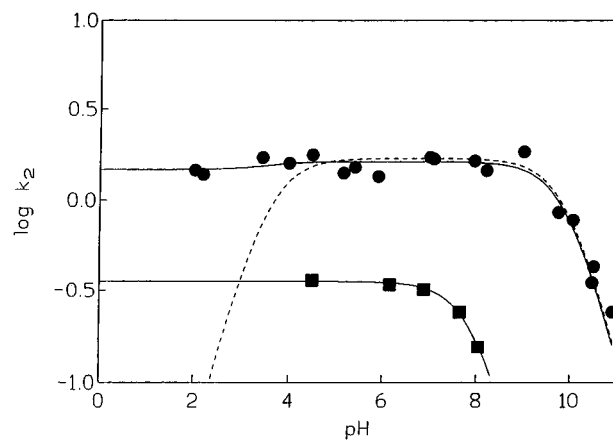


Figure 1. Plots of the second-order rate constants for the attack of thioglycolic acid (**2**, circles) and ethyl mercaptoacetate (**3**, squares) on **1** as a function of pH, $T = 25$ °C. Lines through the data are computed by NLLSQ fitting of the data in Tables 1 and 2 to eqs 1 and 3, respectively. The dashed line through the thioglycolic acid data is a fit excluding the k_2 term in eq 1.

2.75–2.85 (m, 1H, benzylic CH), 3.25–3.36 (m, 2H, NCH_2CH_2), 3.70 (s, 2H, $\text{SCH}_2\text{C}=\text{O}$), 4.19 (q, 2H, CH_2CH_3), 6.48 (d, 1H), 6.62 (d, 1H), 6.96–7.01 (m, 2H); ^{13}C NMR (75 MHz, CDCl_3) δ 14.13, 26.15, 31.34, 31.61, 34.74, 38.22, 41.20, 61.88, 114.27, 116.79, 123.63, 127.25, 129.18, 144.19, 168.79, 197.51; HRMS, exact mass calcd for $\text{C}_{16}\text{H}_{21}\text{O}_3\text{N}_1\text{S}_1$ 307.1242, found 307.1241 (42%).

Results

Given in Table 1 are the second-order rate constants for the reaction of **2** with amide **1** to give the corresponding thio ester **4a**. The identity of that product was deduced from spectral data on material extracted from the reaction mixture. The corresponding kinetic values for the reaction of ethyl 2-mercaptoacetate, **3**, with the amide are given in Table 2; this also gives the corresponding thio ester, **4b**, the identity of which was confirmed by its spectral characteristics and comparison of these with authentic material synthesized by an independent route. The kinetic features of note for these two thiols are evident from the shape of the pH/rate profiles which are given in Figure 1. For thioglycolic acid, looking from high to low pH, the pH/rate profile increases with decreasing pH until the second pK_a of **2** (10.22), after which the profile apparently plateaus down to the lowest pH values that can be reasonably attained (pH 2). In fact, there is an almost imperceptible inflection at the first pK_a of **2** (3.55) followed by another plateau, *vide infra*. In the low-pH region, the values for the rate constants become somewhat uncertain since the background rates for the hydrolysis of **1** are fast, and in the presence of thiol, high absorbencies are encountered. For the ethyl ester **3**, the pH/rate profile increases with decreasing pH until pH 8, the pK_a of the thiol group, and then plateaus in the low pH region.

Given in Table 3 are the rate constants for the reaction of (dimethylamino)ethanethiol (dimethylcysteamine, **5**) with amide **1**. Part of these data were obtained in an earlier study,² but in the present work there was observed a plateau in the low-pH region, (shown in Figure 2), which was not seen before.

In order to check for buffer catalysis, the kinetics of the reaction of **1** with varying [thiol] at known, but constant, concentrations of *N*,2-dimethylimidazole and acetate were determined, the k_2^{obs} values also being given in Tables 1 and 2. Plots of k_{obs} vs [thiol] in the presence of high (0.1–1.0 M) [buffer] were linear, the slopes being independent of [acetate or *N*,2-dimethylimidazole] signifying that there was no inter-

(7) Hall, C. M.; Wemple, J. J. *Org. Chem.* **1977**, *42*, 2118–2123.

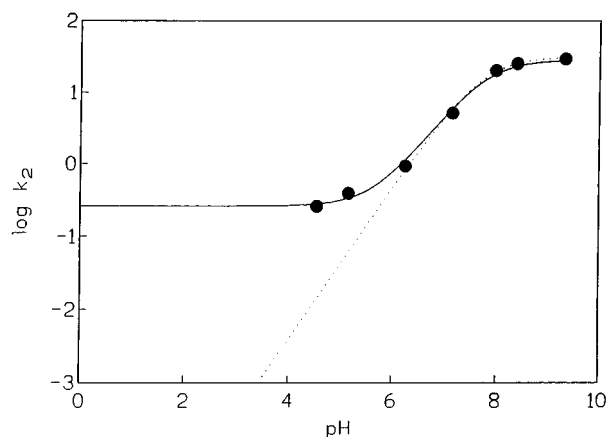
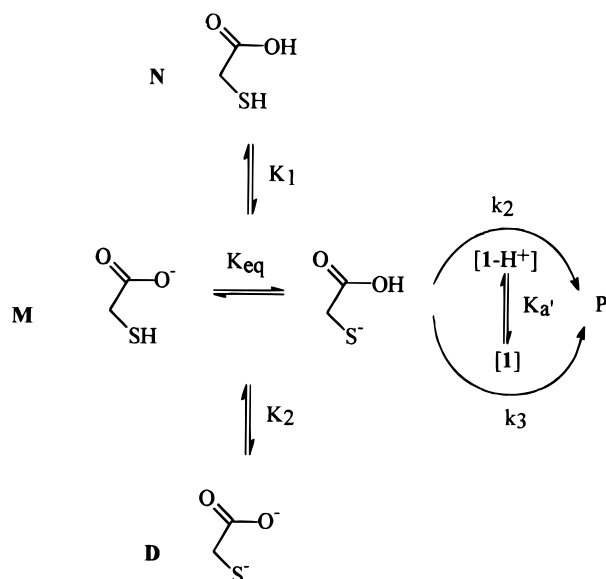


Figure 2. Plot of the second-order rate constant for the attack of dimethylcysteamine (**5**) on **1** as a function of pH, $T = 25\text{ }^{\circ}\text{C}$. The solid line through the data is that computed by fitting the data in Table 3 to eq 4. The dashed line is computed from eq 4 excluding the k_2 term.

Scheme 2



molecular catalysis of the reaction, at least for these two buffers. However, in the presence of *N*-methylimidazole, a different behavior was seen in that plots of k_{obs} vs [2 or 3] showed a curvature as indicated in Figure 3, the kinetic data being given in Tables 1S and 2S, Supporting Information.

Discussion

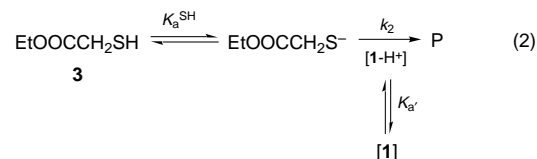
Reaction of Thioglycolic Acid (2) and Ethyl Mercaptoacetate (3) with Amide 1. (i) **Attack of RS^- on 1-H^+ in the Low-pH Region.** The pH rate profile for the reaction of thioglycolic acid (**2**) with amide **1** shown in Figure 1 is consistent with the process shown in Scheme 2 where the monoanionic form of thioglycolic acid, **M**, can react with both neutral and protonated forms of amide **1**. From this scheme the observed rate constant for the appearance of ring-opened product **P** can be written as eq 1, derived for conditions where $[\text{H}^+] \ll K_a'$,

$$k_2^{\text{obs}} = \frac{((k_2/K_a')K_1[\text{H}^+]^2 + k_3K_1[\text{H}^+])}{([\text{H}^+]^2 + K_1[\text{H}^+] + K_1K_2)} \quad (1)$$

where K_1 and K_2 are the first and second macroscopic acid dissociation constants for thioglycolic acid and K_a' is the acid

dissociation constant for the protonated amide. NLLSQ fitting of the data in Table 1 to this equation, after supplying values for K_1 (2.82×10^{-4}),⁷ K_2 (6.02×10^{-11}),⁷ and K_a' (1.9),⁸ yielded the rate constants $k_2 = 9.9 \times 10^3 \text{ M}^{-1} \text{ s}^{-1}$ and $k_3 = 1.63 \text{ M}^{-1} \text{ s}^{-1}$ for attack of the monoanion on 1-H^+ and **1**, respectively. The fit generated by these numbers is shown in Figure 1 as the solid line through the data for **2**. That the appropriate mechanism involves the attack of the monoanionic form of **2** on 1-H^+ is evidenced by the fact that if this term is omitted, the fit to the data (Figure 1, dotted line) is poor in the low-pH region since the predicted rate would have to drop linearly with pH below the first $\text{p}K_a$ of **2** (3.55) if the monoanion can only attack neutral **1**.

For the case of ethyl mercaptoacetate, **3**, the kinetic profile in Figure 1 is consistent with either a process where the neutral thiol reacts with **1** or a more likely kinetic equivalent process shown in eq 2 where the monoanionic thiolate attacks 1-H^+ . Such behavior has some precedence since it is known⁸ that acetate and the monocarboxylate anions of succinic and glutaric acids can react with 1-H^+ . The latter two monoanions are particularly effective as nucleophiles due to the presence of an intramolecular COOH pendant that captures the first formed anhydride intermediate giving a cyclic anhydride (succinic, glutaric) and the hydrolysis product of **1**.



From eq 2 can be derived the kinetic expression given in eq 3, which when fit to the data of Table 2 produces the line through the ethyl mercaptoacetate data shown in Figure 1. The

$$k_2^{\text{obs}} = (k_2/K_a') K_a^{\text{SH}} [\text{H}^+] / (K_a^{\text{SH}} + [\text{H}^+]) \quad (3)$$

computed values for $k_2K_a^{\text{SH}}/K_a'$ and $\text{p}K_a^{\text{SH}}$ are $0.35 \text{ M}^{-1} \text{ s}^{-1}$ and 7.97, the latter dissociation constant agreeing well with the literature value⁵ of 8.02. If one accounts for the values of these two acid dissociation constants, the actual value for k_2 , the rate constant for attack of the monoanion on 1-H^+ , is $6.35 \times 10^7 \text{ M}^{-1} \text{ s}^{-1}$.

The high value for this rate constant invites comparison with the analogous value for the attack of $\text{HOOCCH}_2\text{S}^-$ on 1-H^+ . In principle one expects that there should be no substantial difference in the nucleophilicity of $\text{EtO}_2\text{CCH}_2\text{S}^-$ and $\text{HO}_2\text{CH}_2\text{S}^-$ other than that associated with the minor difference in the $\text{p}K_a'$'s of the thiol. When ionized, the dominant anionic form of **2** is the thiocarboxylate, 2-COO^- , since the carboxylic acid is far more acidic than the SH (see Scheme 3; $\text{p}K_{a1}^{\text{SH}}$ estimated as 8, $\text{p}K_{a1}^{\text{OH}} = 3.55$).⁹ Thus, at any given pH, the ratio⁹ of

(8) Wang et al. (Wang, Q. P.; Bennet, A. J.; Brown, R. S.; Santarsiero, B. D. *J. Am. Chem. Soc.* **1991**, *113*, 5757) have reported the $\text{p}K_a'$ of 1-H^+ to be -0.27 on the basis of an observed curvature in the k_{obs} vs pH profile at high pH.

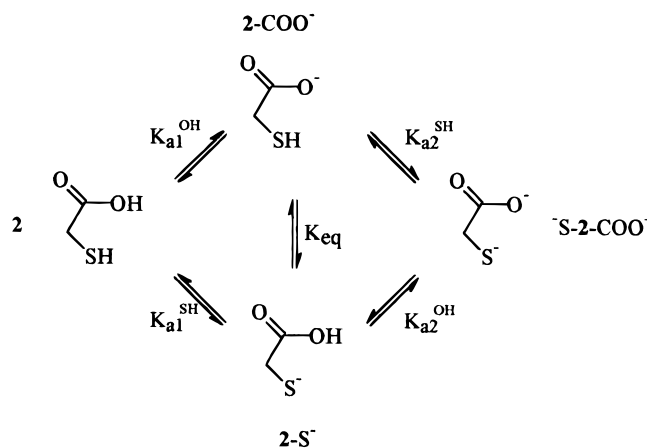
(9) The estimated microscopic $\text{p}K_a'$'s for thioglycolic acid identified in Scheme 3 are based upon the macroscopic $\text{p}K_a$'s for the first ionization of **2**, which is largely attributable to the ionization of the COOH group, and the value for ionization of the SH group in **3** of 8.02⁵ which should be roughly the same as that for the ionization of the SH in thioglycolic acid. Using these two ionization constants, one can calculate the equilibrium constant for $[\text{-OOCCH}_2\text{SH}]/[\text{HOOCCH}_2\text{S}^-] = 2.8 \times 10^4$.

(10) *Merck Index*, 11th ed.; Merck and Co. Inc.: Rahway, NJ, 1989; p 4385.

(11) Kellogg, B. A. Ph.D. Dissertation, University of Alberta, 1995.

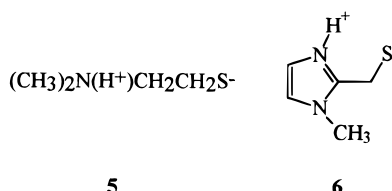
(12) Fersht, A. *Enzyme Structure and Mechanism*, W. H. Freeman and Co.: New York, 1985, pp 147–8.

Scheme 3



$[\text{OOCCH}_2\text{SH}]$ to $[\text{HOOCCH}_2\text{S}^-]$ is roughly 2.8×10^4 . If one quantitatively accounts for the fact that the thiolate represents only a small component of the total monoanionic species, the corrected second-order rate constant for attack of 2-S^- on 1-H^+ is $(9.9 \times 10^3 \text{ M}^{-1} \text{ s}^{-1} \times 2.8 \times 10^4)$ or $2.8 \times 10^8 \text{ M}^{-1} \text{ s}^{-1}$. That this computed value is close to the value determined for attack of 3-S^- on 1-H^+ lends credence to our contention that there are similar mechanisms involving attack of S^- on the protonated amide in operation for the two thiols.

It may be reasonably asked whether other thiols show this same behavior. In earlier studies^{2,15} using β -amino thiols we have observed that dimethylcysteamine (**5**) and 2-mercapto-methyl-*N*-methylimidazole (**6**) react with neutral **1** as their zwitterionic forms in the neutral pH domain. In the case of **5**,



between the its two $\text{p}K_a$'s ($\text{p}K_a^{\text{SH}} = 7.74$ and $\text{p}K_a^{\text{NH}^+} = 10.89$),¹⁵ more than 99.9% of the neutral material exists as the zwitterion. In those studies, we limited the investigation to pH values greater than 6 and there was no indication that the zwitterionic form of either thiol could attack 1-H^+ . In this work, we have extended the study for the reaction of **5** with **1** to lower pH values, the second-order rate constants being given in Table 3. Shown in Figure 2 is the pH/rate profile for that process which clearly shows evidence of a plateau region not seen in the earlier studies.^{2,15} The shape of the profile can be accommodated by the process shown in Scheme 4 for which can be derived the kinetic expression given in eq 4, under the conditions where $[\text{H}^+] \ll K_a'$.

$$k_2^{\text{obs}} = K_a^{\text{SH}}(k_2[\text{H}^+]/K_a' + k_1)/(K_a^{\text{SH}} + [\text{H}^+]) \quad (4)$$

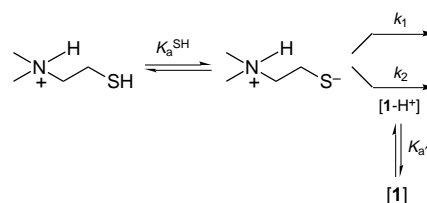
With fixed values for the $\text{p}K_a^{\text{SH}}$ of **5**- H^+ of 7.74¹⁵ and a $\text{p}K_a'$

(13) Hupe and Jencks (Hupe, D.; Jencks, W. P. *J. Am. Chem. Soc.* **1977**, *99*, 451) have shown that the rate constants for acyl transfer from *p*-nitrophenyl acetate to thiol anions have a small sensitivity to the thiol $\text{p}K_a$, $\beta_{\text{nuc}} = 0.27$ for rate-limiting attack of basic thiols. Since the attack on the protonated amide by thiolate is expected to be rate-limiting in our cases, a similar β should be expected.

(14) Nenasheva, T. N.; Salinkove, G. A. *Zh. Org. Khim.* **1979**, *15*, 835.

(15) (a) Keillor, J. W.; Brown, R. S. *J. Am. Chem. Soc.* **1991**, *113*, 5114. (b) In the above study and that reported in ref 2, the reactions of ethanethiol and mercaptopropionitrile could not be observed above the background hydrolysis of **1**. Therefore the k_2^{obs} values quoted here are upper limits.

Scheme 4



for 1-H^+ of -0.27 ,⁸ NLLSQ fitting of the data in Table 3 to eq 4 gives values for the rate constants, $k_1 = (28 \pm 2) \text{ M}^{-1} \text{ s}^{-1}$ and $k_2 = (2.7 \pm 0.3) \times 10^7 \text{ M}^{-1} \text{ s}^{-1}$, respectively. That the latter value is similar to those determined above for thioglycolate and ethyl mercaptoacetate anions supports the general mechanism of S^- attack on 1-H^+ . The variation in the efficacy of 5-S^- , 2-S^- , and 3-S^- is presumably attributable to a complex mixture of effects including differences in $\text{p}K_a$ relating to a Brønsted dependence and structural and solvation differences.

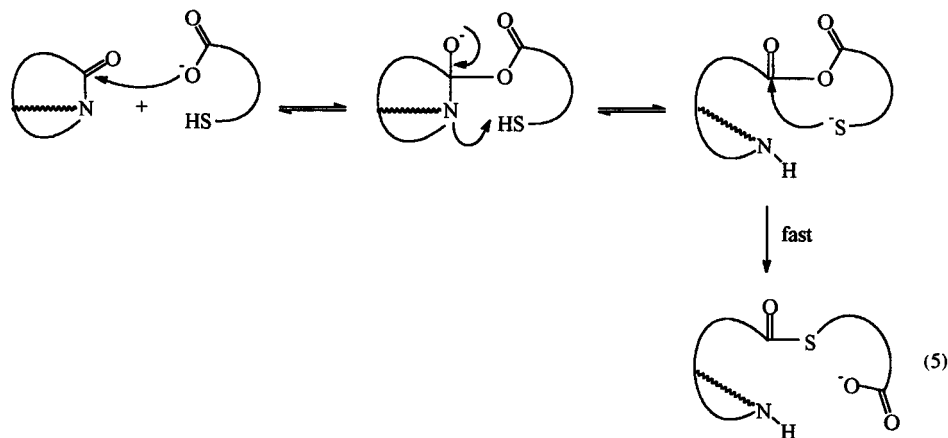
(ii) **Anion Attack on 1 in the Neutral pH Region.** While there is little doubt that the attack of thiolate on 1-H^+ occurs, the plateau region from pH 9 to 4 in the case of thioglycolic acid indicates either that the monoanion of **2** attacks the neutral amide or, alternatively, a kinetically equivalent mechanism involving attack of the dianion of **2** on 1-H^+ could occur. There are a number of possibilities that need to be considered.

(a) **RS^- or RCOO^- Attack.** (1) Although the observed product for the reaction is the thio ester, and our favored process is attack of thiolate on **1**, a possibility exists that the carboxylate could attack **1** as in Scheme 5 to form a transient anhydride intermediate that quickly undergoes intramolecular O to S acyl transfer. Whatever the process is, the second-order rate constant for attack on **1** is $1.63 \text{ M}^{-1} \text{ s}^{-1}$. In this pH region the dominant form is 2-COO^- , but it is difficult to believe that the carboxylate group is the nucleophilic portion. It might be considered that 2-COO^- should be capable of reacting with **1** with a rate similar to that of an unactivated carboxylic acid anion such as CH_3COO^- , but in previous studies,^{3,8} we have been unable to detect any activity for acetate anion on the neutral form of **1**.

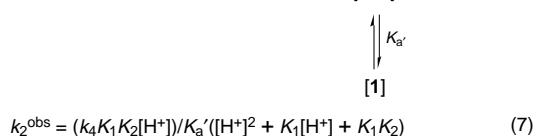
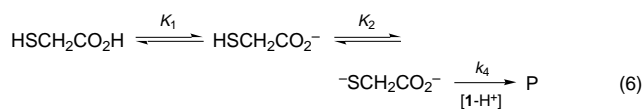
(2) While unactivated COO^- appears not to be nucleophilic enough to account for the observed rate, it may be argued that there is some intramolecular assistance of the attack of the 2-COO^- group by the internal SH pendant, perhaps as a general acid to capture the first formed tetrahedral intermediate thereby driving it toward a transient anhydride product (see Scheme 5). However, if this were so, then it would be reasonably expected that the glycine zwitterion (**7**, $^-\text{O}_2\text{CCH}_2\text{NH}_3^+$), which is isostructural with thioglycolate, and has a similar $\text{p}K_a$ for the pendant NH_3^+ group (9.6^{10} relative to 10.22^5 for the SH in 2-COO^-), also would be substantially reactive with **1**, which it is not.¹¹ Control experiments established¹¹ that at pH 6.18 (MES buffer, 0.2 M) and 7.55 (MOPS, 0.2 M) the second-order rate constants for the glycine attack on **1** are $(6.5 \pm 0.1) \times 10^{-3}$ and $(7.1 \pm 0.3) \times 10^{-3} \text{ M}^{-1} \text{ s}^{-1}$, respectively, these values being 200-fold less than the rate constant observed for attack of thioglycolate. Given the above we conclude that, in the pH region from 4 to 10, attack of thioglycolate on **1** does not proceed through the carboxylate.

(b) **Attack of Dianion of 2 on 1-H^+ .** (1) Although it is unlikely that the reaction proceeds by the attack of 2-COO^- on neutral **1**, a kinetically equivalent process exists wherein $^-\text{SCH}_2\text{COO}^-$ attacks an activated 1-H^+ as in eq 6 for which can be derived the kinetic expression given in eq 7 under

Scheme 5



conditions where $[H^+] \ll K_a'$.



It is reasonable that the reactivity of the COO⁻ portion of the dianion of **2** should be similar to that of **2-COO⁻**. Therefore, on the basis of the pH/rate profile, we can conclude that the COO⁻ portion cannot be the nucleophilic one toward **1-H⁺** since in the region of pH 9–4 where the amount of ionized COO⁻ does not change, the rate would have to increase linearly with falling pH. Thus, in order to account for the possible reaction of the dianion with **1-H⁺**, the attacking atom would have to be S⁻. For this process, the computed second-order rate constant (k_4 in eq 7) would be $5.2 \times 10^{10} \text{ M}^{-1} \text{ s}^{-1}$. This rate constant falls at the higher end expected for a diffusion limited process¹² considering that the reaction involves the diffusion together of an anion of charge -2 and a cation of charge +1. As a result this mechanism cannot be completely ruled out, but it is rendered unlikely on the basis of other factors presented below.

(2) We have already shown above that the reactions of EtO₂CCH₂S⁻ and HOOCCH₂S⁻ with **1-H⁺** proceed with rate constants of 6.35×10^7 and $2.8 \times 10^8 \text{ M}^{-1} \text{ s}^{-1}$. It is difficult to envision any general mechanism by which the pendant carboxylate group could significantly accelerate reaction of the thiolate anion with an already protonated amide. However, there is an increase in the pK_a of the thiolate in HSCH₂COO⁻ relative to those in EtO₂CCH₂SH and HOOCCH₂SH which may result in an increase in the S⁻ nucleophilicity according to a Brønsted relationship.¹³ Therefore, the rate of this process might be expected to be comparable to the rates of the reaction of amide **1** with other thiols which have approximately the same pK_a values. However, such thiols are known to react with amide **1** much slower than does thioglycolic acid. For example, the second-order rate constant for the reaction of CH₃CH₂S⁻ with **1-H⁺** (pK_a of ethanethiol = 10.55¹⁴) is less than $2 \times 10^9 \text{ M}^{-1} \text{ s}^{-1}$ ^{15b} which is more than 20 times lower than the rate constant for the reaction of thioglycolate dianion with **1-H⁺**. The former with its higher pK_a would be expected to be a better nucleophile unless other factors were important. Above we have indicated that there may be some kinetic enhancement of the attack of an anion on a positively-charged substrate. Carriuolo and Jencks have suggested that anions are more reactive toward (+)-charged

acetylimidazolium ion (AI) than they are toward the neutral *p*-nitrophenyl acetate (pNPA).¹⁶ However, the data given¹⁶ suggest that the effects are highly dependent on the nature of the anions. For example, after one accounts for the inherently greater reactivity toward nucleophilic attack of acetylimidazolium relative to pNPA by normalizing the H₂O reaction to a common value, HAsO₄²⁻, HPO₄²⁻, and phenoxide are indeed more reactive toward AI than toward pNPA, but the trend is reversed for acetate, and there is no substantial difference for mercaptoethanol, thioglycolic acid, azide, and hydroxide. Furthermore, if there were a substantial enhancement of the attack of anions on **1-H⁺** then one expects that the rate constant for attack of the zwitterionic, but formally neutral, form of dimethyl cysteamine (**5**, pK_a = 7.74¹⁵) on **1-H⁺** should be substantially less than that for the anion of mercaptopropionitrile (pK_a = 8.74^{15a}) which it is not (k_2 values of $2.7 \times 10^7 \text{ M}^{-1} \text{ s}^{-1}$ and $<2.0 \times 10^7 \text{ M}^{-1} \text{ s}^{-1}$, respectively).^{15b} In the absence of a substantial charge-based enhancement of reactivity, it is unlikely that the dianionic form of thioglycolate is a kinetically important reactant with **1-H⁺**. As a result, we are left with the most favored mechanism in the plateau region being the attack of the monoanionic form of **2** on neutral amide **1**. As will be outlined below, this mechanism is operationally similar to that exhibited by other bifunctional nucleophilic catalysts.^{1–3, 15}

(c) **S⁻ Attack Followed by Intramolecular Trapping of Tetrahedral Intermediate by COOH.** Given in Scheme 6 is a pathway that is most consistent with the available data for the attack of the anions of **2** and **3** on **1** in the neutral pH region. Scheme 6 is a more detailed extension of Scheme 2 in that it includes the formation of various intermediates following the nucleophilic attack of the S of **2⁻** on **1**. Whether the attack occurs unassisted as **2-S⁻** or as a general base assisted attack of SH by the intramolecular COO⁻ in **2-COO⁻** cannot be ascertained from the available information. However, we note that for the reaction of thiols with an activated ester such as *p*-nitrophenyl acetate where the rate-limiting step is known to be attack, general base assistance is not observed, and the attack occurs unassisted via thiolate anion.^{6a,17} On this basis, our preferred mechanism for the formation of **T_O⁻** involves unassisted attack of **2-S⁻** on **1**. The process shown in Scheme 6 is directly analogous to that presented earlier^{2,15a} for the attack of zwitterionic ammonium thiolates on **1**. Following that analysis, we assume that thiolates in general are capable of attacking **1** to form a tetrahedral intermediate (**T_O⁻**). However,

(16) (a) Jencks, W. P.; Carriuolo, J. *J. Am. Chem. Soc.* **1960**, *82*, 1778. (b) Jencks, W. P.; Carriuolo, J. *J. Biol. Chem.* **1959**, *234*, 1272, 1280.

(17) (a) Schonbaum, G. R.; Bender, M. L. *J. Am. Chem. Soc.* **1969**, *82*, 1900. (b) Fersht, A. R. *J. Am. Chem. Soc.* **1971**, *93*, 3504. (c) Barnett, R. E.; Jencks, W. P. *J. Am. Chem. Soc.* **1967**, *89*, 5963; **1969**, *91*, 2358.

Scheme 6

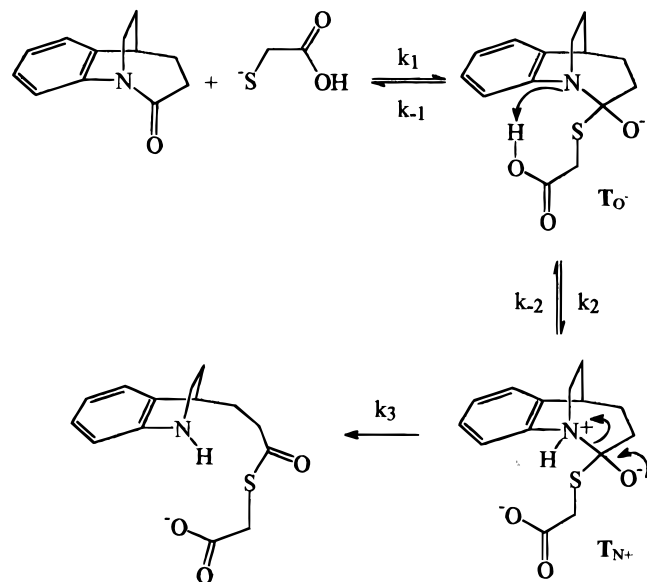


Table 4. Second-Order Rate Constants for the Attack of a Variety of Bifunctional and Other Nucleophiles on Amide **1** in H₂O, *T* = 25 °C

nucleophile	k_2^{\max} (1) (M ⁻¹ s ⁻¹)	k_2^{\max} (1-H ⁺) (M ⁻¹ s ⁻¹)
OH ⁻ ^a	60	n.o.
H ₂ O	n.o.	106 ^f
6 ^b	100	g
5 ^b	28	2.7 × 10 ⁷ ^e
(CH ₃) ₂ NCH ₂ CH ₂ OH ^c	0.25	n.o.
CH ₃ COO ⁻	n.o.	3.7 × 10 ² ^{f,h}
HO ₂ C(CH ₂) ₃ COO ⁻ ^d	0.26	1.47 × 10 ⁴ ^d
HO ₂ C(CH ₂) ₂ COO ⁻ ^d	0.27	2.56 × 10 ⁴ ^d
EtO ₂ CCH ₂ S ⁻ ^e	n.o.	6.35 × 10 ⁷ ^e
HO ₂ CCH ₂ S ⁻ ^e	4.6 × 10 ⁴	2.8 × 10 ⁸ ^e
<i>N</i> -methylimidazole	0.03–0.04 ⁱ	

^a Reference 1c, n.o. = not observed. ^b Reference 2 and 15. ^c Reference 1a,b. ^d Reference 3. ^e This work. ^f Reference 8. ^g Probably comparable to that for **5** but not determined. ^h Does not act as a nucleophile, but rather as a general base for delivery of H₂O to **1-H**⁺. ⁱ From fits to eq 9

it is only the thiolates which contain a general acid pendant (such as COOH, or >NH⁺¹⁵) that are capable of converting **T**_O⁻ into **T**_N⁺ which is almost certainly the form required for rapid breakdown to product **4a**. One can gain an appreciation of the effectiveness of the overall process for **2-S**⁻ by correcting the observed rate constant of 1.63 M⁻¹ s⁻¹ for the amount of the species present as thiolate monoanion,⁹ e.g. [HSCH₂CO₂⁻]/[⁻SCH₂CO₂H] = 2.8 × 10⁴. Thus, the true second-order rate constant for the reaction of **2-S**⁻ with **1** is (1.63 M⁻¹ s⁻¹ × 2.8 × 10⁴) or 4.6 × 10⁴ M⁻¹ s⁻¹.

Listed in Table 4 are the second-order rate constants for the attack on **1** by a variety of anionic, zwitterionic, and neutral nucleophiles. That several of the species such as **2**, **5**, and **6** are in fact as, or more, reactive than the strong nucleophile OH⁻ is a consequence of the bifunctional nature of the nucleophiles which permits trapping of the unstable tetrahedral intermediate subsequent to the attack of the nucleophile as in Schemes 1 and 6. Interestingly, **2-S**⁻ is the most reactive species toward neutral **1** that we have found. This may be a result of the fact that the proton transfer from the COOH pendant to the anilino N in **T**_O⁻ (Scheme 6) is thermodynamically favorable, and therefore fast enough to preclude reversal via *k*₋₁ such that the rate-limiting step is exclusively nucleophilic attack. In the case of the reaction of ammonium thiolates with **1**, proton transfer

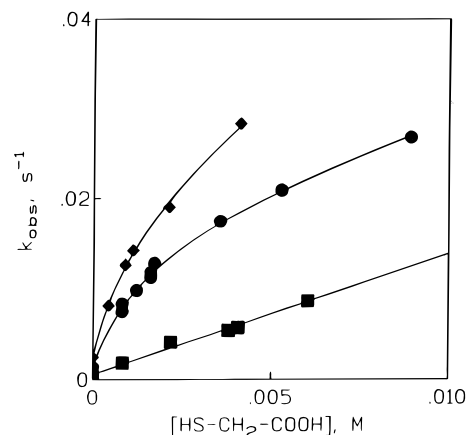
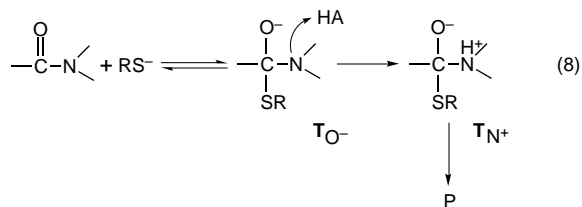


Figure 3. Plots of k_{obs} vs $[\mathbf{2}]_{\text{total}}$ for the reaction with **1** at various [*N*-methylimidazole], pH = 7.2, μ = 1.0 (KCl), *T* = 25 °C: diamonds, [*N*-methylimidazole]_{total} = 0.6 M; circles, [*N*-methylimidazole]_{total} = 0.4 M; squares, [*N*,2-dimethylimidazole]_{total} = 1.0 M. The lines through the data are computed by fitting the data in Tables 1S and 2S to eq 9. The straight line shows the dependence in the presence of *N*,2-dimethylimidazole.

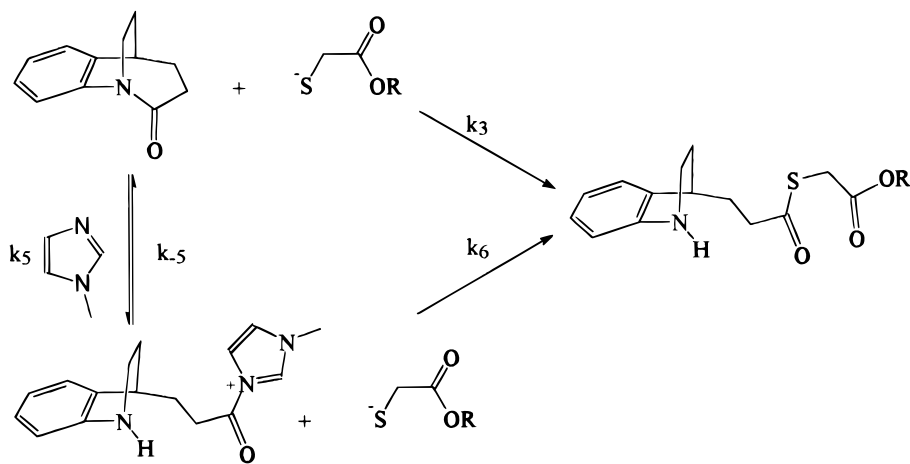
from a more weakly acidic ammonium group in **T**_O⁻ to the anilino N is thermodynamically less favorable and therefore slower which may allow reversal to occur prior to trapping so that the rate limiting step is a composite of *k*₁ and *k*₂. In our previous study,¹⁵ we have noted that the reaction of morpholinoethanethiolate zwitterion with **1** exhibits substantial general acid catalysis by added *N*-methylimidazolium consistent with *intermolecular* trapping of the **T**_O⁻ which would be consistent with a two-step process where the second step is rate limiting or partially so.

This raises a reasonable question as to whether it is possible that an analogous *intermolecular* general acid catalysis of the reaction of **2-S**⁻ with **1** can be observed. Indeed, our preferred mechanism for the attack of thiolate anion on **1-H**⁺ (such as for **3** and **5** and also in the low pH region for **2**) has a kinetic equivalent wherein the anions attack the neutral form of **1** followed by rate-limiting capture of the unstable tetrahedral intermediate by H₃O⁺ as in eq 8.



In order to probe this question, we studied the effect of 0.1 and 1.0 M acetate on the second-order rate constants for attack of **3** and **5** on **1-H**⁺ at pH 4.51–4.54 and 1.0 M *N*,2-dimethylimidazole on the reaction of **2** with **1** at pH 7.20 (see entries in Tables 2 and 3). In no case did we observe that the attack of these species was enhanced by the presence of high concentrations of these buffers. This indicates first that *intermolecular* catalysis of the type suggested in eq 8 is inefficient and that at low pH **3** and **5** must react with an already protonated **1-H**⁺. Second, in the case of the reaction of **2** with **1**, the absence of *intermolecular* general acid catalysis can indicate that the rate-limiting step is simply *k*₁ with a subsequent fast proton transfer from the COOH, unlike the situation with the ammonium thiolates where the presence of general acid catalysis indicates that the proton transfer to trap **T**_O⁻ is at least partially rate limiting.¹⁸

Scheme 7



(R refers to H in case of **2** and Et in case of **3**)

(d) Nucleophilic Catalysis of the Reaction of **2 and **3** with **1** by *N*-Methylimidazole.**

Although intermolecular general catalysis of the reaction of thiols with **1** is not an observed process, there is one piece of evidence that indicates that intermolecular nucleophilic catalysis of the thiolate reaction is a facile process. Shown in Figure 3 are plots of the k_{obs} values vs $[\text{thioglycolate}]_{\text{total}}$ at various concentrations of *N*-methylimidazole, pH 7.2, the primary data being given in Table 1S (Supporting Information). The nonlinear behavior of the kinetics arises from a superposition of two processes for the disappearance of **1** which is simply fit by the process given in Scheme 7. One of these processes gives the linear dependence of k_{obs} on $[\mathbf{2}]$ which is described above as occurring in the absence of *N*-methylimidazole. The other is a saturation process wherein *N*-methylimidazole reversibly attacks **1** to form a transient *N*-acylimidazolium cation which is subsequently captured by thioglycolate. For the process depicted in Scheme 7 can be derived the kinetic expression given in eq 9, and NLLSQ fitting of each set of data in Table 1S to this expression yields the lines through the data in Figure 3 and the associated rate constants: $k_3 = 1.3\text{--}1.7 \text{ M}^{-1} \text{ s}^{-1}$, $k_5 = 0.03\text{--}0.04 \text{ M}^{-1} \text{ s}^{-1}$, and $k_{-5}/k_6 = 1.0 \times 10^{-3} \text{ M}$.

$$k_{\text{obs}} = \frac{k_3[\mathbf{2}] + (k_5 k_6 [\textit{N}\text{-methylimidazole}][\mathbf{2}])}{(k_{-5} + k_6 [\mathbf{2}])} \quad (9)$$

For this process, the saturation behavior is a reflection of the fact that at low $[\mathbf{2}]$, there is a rapid pre-equilibrium for the addition of the imidazole with a slow second step (k_6), while at high $[\mathbf{2}]$, the k_5 step is rate limiting. Also shown in Figure 3 is a k_{obs} vs $[\text{thioglycolate}]_{\text{total}}$ relationship in the presence of *N*,2-dimethylimidazole. The latter imidazole has no effect on this process, and in fact the data lie on the same line determined in the absence of *N*,2-dimethylimidazole. This observation strongly supports the nucleophilic role proposed above for *N*-methylimidazole. Since it is well-established that the nucleophilicity of *N*,2-dimethylimidazole is suppressed by the presence of the 2-CH₃ group,¹⁹ a much smaller value for its k_5 term is expected, in agreement with the observed dependence in Figure 3.

It is reasonably expected that a similar catalytic involvement of *N*-methylimidazole can be observed for the attack of other thiols on **1**. Shown in Figure 4 is a comparison of the plots of

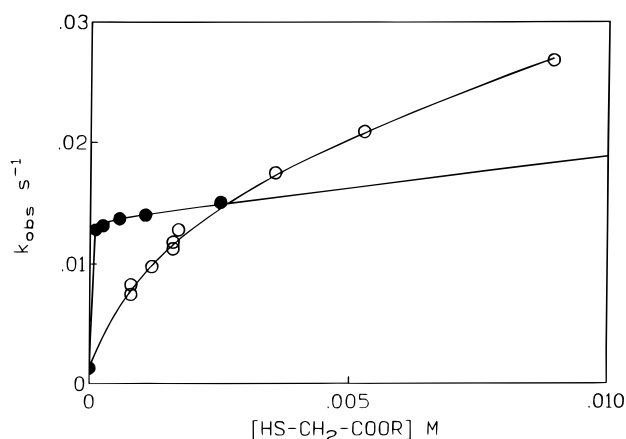


Figure 4. Plots of k_{obs} vs $[\mathbf{2}]$ (open circles) and $[\mathbf{3}]$ (closed circles) for their reaction with **1** in the presence of 0.4 M *N*-methylimidazole, $T = 25 \text{ }^\circ\text{C}$, $\text{pH} = 7.2$, $\mu = 1.0$ (KCl).

k_{obs} vs thiol for **2** and **3** in the presence of 0.4 M *N*-methylimidazole (data for **3** from Table 2S, Supporting Information). Although the profiles for the two thiols are somewhat different, both adhere to the common mechanism given in Scheme 7. The main difference is that saturation occurs sooner with ethyl mercaptoacetate than with thioglycolate, which is largely a manifestation of the greater amount of RS^- of the former at a given pH. NLLSQ fitting of the ethyl mercaptoacetate data of Table 2S (Supporting Information), to eq 9 gives the partitioning of the acylimidazolium as $k_{-5}/k_6 = 6 \times 10^{-6} \text{ M}$. Considering that the k_{-5} process should be independent of the nature of the thiolate, the main difference in the partitioning should then relate to the amount of free RS^- and small differences in the nucleophilicity.¹³ The 160-fold difference in the k_{-5}/k_6 ratio for the process with **2** and **3** is easily accommodated by the difference in the concentrations of the thiol anions resulting from the difference in their pK_a 's (8.0 for **3** and 10.22⁵ for **2**). Finally, the observation that the k_{-5}/k_6 ratio is insensitive to whether the attacking species is $^-\text{SCH}_2\text{COO}^-$ or $^-\text{SCH}_2\text{COOEt}$ indicates that the reaction is not enhanced by additional ($-$) charge on the thiolate, consistent with arguments presented above in subsection b2.

Two additional points consistent with the mechanism proposed stem from the plots depicted in Figure 4. First, the slopes of the limiting linear portion of the plots gives the limiting values for the reaction of **2** and **3** with **1** in the absence of the imidazole as was discussed above. The computed values are 1.69 and $0.6 \text{ M}^{-1} \text{ s}^{-1}$, close to what was obtained from analysis of the

(18) We thank a referee of an earlier version of this manuscript for this suggestion.

(19) Bender, M. L. *Mechanisms of Homogeneous Catalysis From Protons to Proteins*; Wiley-Interscience: New York, 1971; pp 147–176.

data in Tables 1 and 2. Second, extrapolation of the linear portion of both lines to the *Y*-axis should relate to the value for k_5 , the rate constant for attack of *N*-methylimidazole, which is expected to be the same for the two thiols as is observed ($k_{\text{obs}} = 0.012 \text{ s}^{-1}$, $k_5 = k_{\text{obs}}/[\text{imidazole}] = 0.03 \text{ M}^{-1} \text{ s}^{-1}$ for both **2** and **3**). Such consistency of the results provides convincing corroboration of the validity of the proposed mechanism.

Conclusions

Previous studies explored the propensity of **1** to react with bifunctional nucleophiles that were considered as biomimics of the active site residues in proteases. The current study has shown a non-biomimetic bifunctional nucleophilic species, thioglycolate, as its $^-\text{SCH}_2\text{COOH}$ form is also active toward **1**. This further illustrates that the general features that are necessary for activity of such species toward **1** and presumably other amides⁴ include a powerfully nucleophilic component and an acidic pendant capable of transferring a proton to trap an unstable tetrahedral intermediate. The importance of this latter feature is illustrated from the observations that powerfully nucleophilic thiolates that do not possess the intramolecular general acid pendant are incapable of productively reacting with neutral **1**, nor are these reactions subject to marked intermolecular general acid catalysis. Rather, the most efficient mechanism by which such thiolates can react is via attack on the already protonated form of **1**, thereby avoiding the catalytic task of having to trap, by general acid protonation, an unstable

intermediate whose overwhelmingly favorable pathway for breakdown is reversion to starting material. The data of Table 4 also show that all thiols we have investigated have a large tendency to attack **1**-H⁺ with second-order rate constants on the order of 10^7 – $10^8 \text{ M}^{-1}\text{s}^{-1}$. However, in practice these pathways are inefficient at neutrality for most thiols due to the mutually incompatible pH dependencies of the concentrations of the essential species, RS⁻ and **1**-H⁺.

Acknowledgment. We gratefully acknowledge the financial assistance of the University of Alberta, where the initial studies were done, and the Natural Sciences and Engineering Research Council of Canada. In addition, B.A.K. acknowledges the Alberta Heritage Medical Research Foundation for a postgraduate fellowship. Finally, the authors acknowledge the assistance of Dr. D. Gallagher and Mr. M. Howrsh who, at the University of Alberta, performed initial studies of the reaction of **1** with **2**.

Supporting Information Available: Table 1S (observed pseudo-first-order rate constants for the reaction of **2** with amide **1** at various concentrations of *N*-methylimidazole buffer) and Table 2S (observed pseudo-first-order rate constants for the reaction of **3** with amide **1** at various concentrations of *N*-methylimidazole buffer (2 pages). See any current masthead page for ordering and Internet access instructions.

JA961312Y